HHS Public Access

Author manuscript

J Proteomics. Author manuscript; available in PMC 2018 August 23.

Published in final edited form as:

J Proteomics. 2017 August 23; 166: 127–137. doi:10.1016/j.jprot.2017.07.008.

A mass spectrometry-based proteomic analysis of Homer2-interacting proteins in the mouse brain

Scott P. Goulding[*,1,2,3,4], **Karen K. Szumlinski**[5], **Candice Contet**[1], **Michael J. MacCoss**[4], and **Christine C. Wu**[3]

[1]Department of Neuroscience, The Scripps Research Institute, La Jolla, CA

[2]Neuroscience Program, University of Colorado Anschutz Medical Campus, Aurora, CO

[3]Department of Cell Biology, University of Pittsburgh School of Medicine, Pittsburgh, PA

[4]Department of Genome Sciences, University of Washington, Seattle, WA

[5]Department of Psychological and Brain Sciences, Molecular, Cellular and Developmental Biology, and The Neuroscience Research Institute, University of California, Santa Barbara, Santa Barbara, CA

Abstract

In the brain, the Homer protein family modulates excitatory signal transduction and receptor plasticity through interactions with other proteins in dendritic spines. Homer proteins are implicated in a variety of psychiatric disorders such as schizophrenia and addiction. Since Homers serve as scaffolding proteins, identifying their interaction partners is an important first step in understanding their biological function and could help design novel therapeutic strategies. The present study set out to document Homer2-interacting proteins in the mouse brain using a co-immunoprecipitation-based mass spectrometry approach. *Homer2* knockout samples were used to filter out non-specific interactors. We found that in the brain, Homer2 interacts with a limited

[*]Corresponding author: Scott P. Goulding, Ph.D., Postdoctoral Fellow, Contet Lab, The Scripps Research Institute, Department of Neuroscience, 10550 North Torrey Pines Road, SP-273, La Jolla, CA 92037, goulding@scripps.edu, Office: (858) 784-9041, Cell: (707) 696-6567, Fax: (858) 784-8851.

Data availability: We made all RAW mass spectrometry data files available as part of the Chorus Project. To download RAW files, follow these links:

For the Homer2 co-IP experiment: https://chorusproject.org/anonymous/download/experiment/f278cd19a9b24d98bab551be4079d428

For the Homer2 co-IP verification experiment: https://chorusproject.org/anonymous/download/experiment/4614a5f2727c4052887df68b 10bc4b2f

We also made the "Supplemental Data 1-3" Skyline documents available through Panorama. To view, please follow this link: https://panoramaweb.org/labkey/homer2_interactome.url
Reviewer account access: panorama+maccoss2@proteinms.net, Password: H=Etd5ne
Currently, it is not possible to differentiate peptide identification events from MS1 full-scan filtered peptides on the Panorama website. To view peptide identification events, please download the Skyline documents through Panorama and open with Skyline (version 3.5 or newer). Skyline is a vendor-neutral open source quantitation program for mass spectrometry data that is freely downloadable at: https://skyline.gs.washington.edu/labkey/project/home/software/Skyline/begin.view
Note: most of this work was published in the Ph.D. dissertation of Scott P. Goulding for the Neuroscience Program at The University of Colorado, Anschutz Medical Campus.

subset of its previously reported interaction partners (3 out of 31). Importantly, we detected an additional 15 “novel” Homer2-interacting proteins, most of which are part of the N-methyl-D-aspartate receptor signaling pathway. These results corroborate the central role Homer2 plays in glutamatergic transmission and expand the network of proteins potentially contributing to the behavioral abnormalities associated with altered Homer2 expression.

Graphical abstract

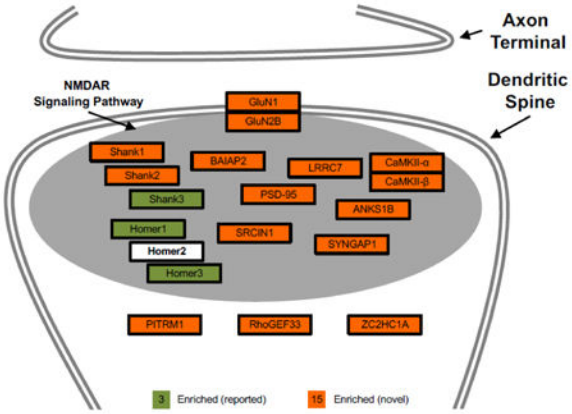

Keywords

Homer2; NMDAR; co-immunoprecipitation; mass spectrometry; MS1 full-scan filtering; Skyline

1. Introduction

In excitatory synapses of the central nervous system, Homer proteins constitute a family of adaptor/scaffolding proteins that regulate excitatory signal transduction and receptor plasticity in dendritic spines by tethering critical effectors into functional complexes at the postsynaptic density (PSD) (reviewed in [1]). Mammalian Homer proteins are the products of three independent genes, *Homer1-3*. Homers share two main structural features: a well conserved amino-terminal class II Enabled/vasodilator-stimulated phosphoprotein homology 1 (EVH1) domain [2-6] and a less conserved carboxyl-terminal coiled-coil domain, which is absent from short isoforms (e.g., Homer1a) [4,5,7-11].

Each structural domain has well documented molecular functions: the EVH1 domain binds specific proline-rich consensus sequences (i.e. PPXXF and PXXF where X is any amino acid, as well as LPSSP) found in numerous proteins [6,12-17] and the coiled-coil domain facilitates longer Homer protein multimerization and the formation of protein scaffolds [4,5,7-11]. Long Homer proteins are constitutively expressed at different levels throughout the brain [4,18] and are concentrated at the PSD below the dense core [19]. In contrast, the short Homer1 proteins (Homer1a and Ania3) are expressed as delayed immediate early genes in an activity-dependent manner and disrupt the protein clusters formed by longer Homers at the PSD [2,3,20]. Homer proteins contribute to the formation and morphological plasticity of dendritic spines [21-24]. Also, by tethering metabotropic glutamate receptors to

intracellular signaling effectors and ion channels, Homers play a critical role in regulating signal transduction at the PSD [1,25]. At the behavioral level, Homer proteins have been implicated in a variety of pathological states such as neuropathic pain [26], schizophrenia [27], and addiction [28-32]. In particular, Homer2 proteins promote excessive alcohol consumption [33-37].

Since Homers function as scaffolding proteins, identifying their interaction partners is a crucial step in understanding the molecular mechanism by which they impact neuronal activity and behavior. For Homer2, a total of 31 interaction partners have been reported in the literature (Supplemental Table S1). However, the interactions of these proteins with Homer2 were characterized by various experimental approaches using different organisms and tissue types. In the present study, we sought to identify the proteins that specifically interact with Homer2 in the mouse brain. To this purpose, we performed Homer2 co-immunoprecipitation (co-IP) experiments in whole brains collected from wild-type (WT) and *Homer2* knockout (KO) mice, analyzed the samples by nano liquid chromatography-tandem mass spectrometry (nLC-MS/MS) followed by MS1 full-scan filtering, and identified co-immunoprecipitated (co-IPed) proteins that were significantly enriched in WT versus KO samples (hereafter referred to as *Homer2 co-IP experiment*). Next, we verified the co-IPed proteins using selected reaction monitoring (SRM) mass spectrometry in a separate Homer2 co-IP experiment (hereafter referred to as *Homer2 co-IP* ***verification*** *experiment*). Overall, analyses revealed that the interactome of Homer2 proteins in the mouse brain minimally overlaps with the set of proteins that had been previously reported in the literature. Importantly, we identified 15 novel interactors that are part of the N-methyl-D-aspartate receptor (NMDAR) signaling pathway, and that may, therefore, contribute to the effects of Homer2 deletion and overexpression on behavioral phenotypes.

2. Materials and methods

2.1 Mouse brain tissue

For the Homer2 co-IP experiment, whole brains were harvested from three male WT (background: 129X1/SvJ X C57BL/6J) and three *Homer2* KO mice [38] (ages 1-5 months) bred in-house by Dr. Szumlinski. For the Homer2 co-IP verification experiment, whole brains were harvested from three male NIA C57BL/6 mice (3 months) purchased from Charles River Laboratories (Seattle, WA). All mice were handled and sacrificed by the guidelines provided by the Institutional Animal Care and Use Committees at the University of California, Santa Barbara and the University of Washington. All brains were stored at -80 °C before use.

2.2 Homer2 co-IP

For the Homer2 co-IP experiment (Figure 1A), whole brains were homogenized separately using a 15 ml Potter-Elvehjem tissue grinder with PTFE pestle (Wheaton Science Products, Millville, NJ) over wet ice in 12 ml of a co-IP buffer containing 20 mM Tris-Cl pH 7.4, 137 mM NaCl, 10% (v/v) glycerol, 1% (v/v) Triton X-100, 2 mM EDTA, and 1X Halt protease and phosphatase inhibitor cocktail (Thermo Fisher Scientific, Rockford, IL). The homogenates were transferred to 15 ml conical tubes and mixed end-over-end for 30 min at

4 °C, then aliquoted into 1.7 ml tubes and centrifuged at 500 × g at 4 °C for 10 min to remove unlysed cells and nuclear material. The supernatants were recombined into new 15 ml conical tubes, mixed by vortexing, and kept on wet ice while protein concentrations were assessed by DC protein assay (Bio-Rad Laboratories, Hercules, CA) according to manufacturer's recommendations. Next, 500 μg of each supernatant was added to 1.7 ml tubes and diluted to 500 μg/1,000 μl with co-IP buffer containing inhibitors. The samples were pre-cleared with 10 μg of an unconjugated rabbit anti-mouse IgG Fc secondary antibody (product # 31194, Thermo Fisher Scientific, Rockford, IL) and 100 μl of equilibrated Invitrogen Protein A-Sepharose 4B Conjugate beads (Life Technologies, Grand Island, NY) by nutating at 4 °C for 30 min and 6 h, respectively. The beads were pelleted by centrifuging twice at 500 × g at 4 °C for 2 min, and the pre-cleared supernatants were transferred to new 1.7 ml tubes after each spin. The samples were co-IPed with 10 μg of a rabbit polyclonal anti-Homer2 antibody (catalog # 160 203, Synaptic Systems, Göttingen, Germany) and 100 μl Protein A-Sepharose 4B Conjugate beads by nutating at 4 °C for 12 h and 6 h, respectively. The beads were pelleted by centrifuging at 425 × g at 4 °C for 2 min, the supernatants were removed, and the beads were washed by nutating three times with 1 ml of co-IP buffer without inhibitors at room temperature for 10 min. The co-IPed proteins were eluted by mixing the beads three times with 100 μl of 200 mM glycine pH 2.5 using a Labquake tube shaker/rotator (Thermo Fisher Scientific, Rockford, IL) at room temperature for 10 min. The eluates were transferred to new 1.7 ml tubes, and the pH was neutralized with equal volumes of 1 M Tris-Cl pH 8. During both washing and elution steps, the beads were pelleted by centrifuging at 425 × g at room temperature for 2 min. Finally, co-IPed proteins were purified by methanol/chloroform precipitation [39] and stored in methanol at -80 °C.

For the Homer2 co-IP verification experiment, the same procedure was used, but protein concentrations were assessed by BCA protein assay (Thermo Fisher Scientific, Rockford, IL) according to manufacturer's recommendations and WT negative control samples were co-IPed with 10 μg of a rabbit polyclonal anti-HA-tag antibody (catalog # 245 003, Synaptic Systems, Göttingen, Germany).

2.3 1-D and 2-D gel electrophoresis

The homogenate, supernatant (hereafter referred to as *input fraction*), pre-cleared input, and co-IP input fractions were purified by methanol/chloroform precipitation. All fractions, including the co-IP sample, were solubilized in 1% SDS by sonication and heating at 60 °C for 30 min. Protein concentrations were determined by DC protein assay (Bio-Rad Laboratories, Hercules, CA). Samples destined for 1-D gel electrophoresis were mixed with SDS gel-loading buffer to reach a final concentration of 50 mM Tris-Cl pH 6.8, 2% SDS, 10% (v/v) glycerol, 0.1% (w/v) bromophenol blue, and 1.25% (v/v) β-mercaptoethanol, heated at 100 °C for 5 min, and stored at -20 °C. Samples destined for 2-D gel electrophoresis or mass spectrometry analysis were purified again by methanol/chloroform precipitation and stored in methanol at -80 °C.

For 1D gel electrophoresis, 10 μg of sample in SDS gel-loading buffer and 10 μl of the Bio-Rad Kaleidoscope protein standard (Bio-Rad Laboratories, Hercules, CA) were loaded into

hand-poured 10% Tris-glycine SDS-polyacrylamide gels topped with a 5 % stacking gel and electrophoresed at 60 V and 100 V through the stacking and resolving gels, respectively, using a Mini-PROTEAN Tetra Cell electrophoresis apparatus (Bio-Rad Laboratories, Hercules, CA). The proteins were either transferred to a PVDF Immobilon-P membrane (Merck Millipore, Billerica, MA) using a Mini Trans-Blot cell (Bio-Rad Laboratories, Hercules, CA) running at 350 mA for 1 h for immunoblotting or prepared for silver staining.

For 2-D gel electrophoresis, proteins were prepared as described by Wu *et al.* [40]. Briefly, 30 μg of protein was solubilized by vortexing in 75 μl of a solution containing 35 mM Tris-base, 9 M urea, 4% (w/v) CHAPS, and 65 mM DTT and 75 μl of a second solution containing 7 M urea, 2 M thiourea, 4% (w/v) CHAPS, 100 mM DTT, 2% (v/v) Pharmalyte broad range pH 3-10 carrier ampholytes (GE Healthcare Bio-Sciences, Pittsburgh, PA), and 0.05% (v/v) bromophenol blue. Immobiline DryStrip gels (7 cm pH 3-10; GE Healthcare Bio-Sciences, Pittsburgh, PA) were rehydrated overnight at room temperature with the solubilized proteins and transferred to a Multiphor II electrophoresis system attached to a MultiTemp III thermostatic chiller and EPS 3501 power supply (GE Healthcare Bio-Sciences, Pittsburgh, PA). The gel strips were covered with mineral oil and electrophoresed at 350 V, 750 V, 1200 V, 2000 V, and 3000 V for 1 h at each voltage then at 3500 V for 41 h at a constant temperature of 15 °C. Next, the gel strips were submerged for 10 min in 1 ml of a reducing solution containing 50 mM Tris-Cl pH 6.8, 6 M urea, 70 mM SDS, 15 % (v/v) glycerol, and 60 mM DTT. The gel strips were submerged for another 10 min in 1 ml of an alkylating solution containing 50 mM Tris-Cl pH 6.8, 6 M urea, 70 mM SDS, 15 % (v/v) glycerol, 68 mM 2-iodoacetamide, and 0.05% (v/v) bromophenol blue. The gel strips were loaded into hand-poured 10% Tris-glycine SDS-polyacrylamide gels topped with a 5 % stacking gel and electrophoresed at 60 V and 100 V through the stacking and resolving gels, respectively, using a Mini-PROTEAN Tetra Cell electrophoresis apparatus (Bio-Rad Laboratories, Hercules, CA). 10 μg of protein purified from the input fraction was included in a lane alongside the gel strips. The proteins were transferred to a PVDF Immobilon-P membrane (Merck Millipore, Billerica, MA) using a Mini Trans-Blot cell (Bio-Rad Laboratories, Hercules, CA) running at 350 mA for 1 h.

2.4 Western blotting

Membranes were blocked for 1 h at room temperature in a buffer containing 10 mM Tris-Cl pH 8, 150 mM NaCl, 0.05% (v/v) Tween 20, and 5 % (w/v) nonfat instant dry milk, then incubated overnight at 4 °C in blocking buffer containing 0.02% (v/v) sodium azide and a 1:1,000 dilution of rabbit anti-Homer2 antibody (catalog # 160 203, Synaptic Systems, Göttingen, Germany) from a 1 μg/μl stock. Next, the membranes were washed at room temperature three times 10 min with blocking buffer, incubated for 2 h at room temperature in blocking buffer containing a 1:20,000 dilution of anti-rabbit IgG (H+L) horseradish peroxidase-conjugated antibody (catalog # W4011, Promega, Madison, WI) from a 1 μg/μl stock, then washed at room temperature three times 10 min with blocking buffer without milk. Finally, membranes were bathed with 1 ml of SuperSignal West Pico Chemiluminescent Substrate (Thermo Fisher Scientific, Rockford, IL), exposed onto Classic BX Autoradiography Film (MIDSCI, St. Louis, MO), and developed using an SRX-101A Film Processor (Konica Minolta, Ramsey, NJ).

2.5 Silver staining

After 1-D gel electrophoresis, the gel was rinsed in water for 5 min and soaked overnight at room temperature in a fixing solution containing 40% (v/v) methanol and 10% (v/v) acetic acid. The gel was rinsed in water for 5 min, soaked for 15 min in a solution containing 0.5 M sodium acetate and 0.16% (v/v) glutaraldehyde, then rinsed three times in water for 10 min. Subsequently, the gel was soaked twice for 15 min in a solution containing 1.5 mM 2,7-naphthalenedisulfonic acid then rinsed four times in water for 10 min. Next, the gel was soaked for 30 min in a silver solution containing 47 mM silver nitrate, 0.4% (v/v) ammonium hydroxide, and 0.024 N sodium hydroxide, then rinsed four times with water for 5 min. Finally, the gel was soaked in a developing solution containing 0.26 mM citric acid and 0.037% (v/v) formaldehyde before the reaction was quenched by soaking the gel for 5 min in a solution containing 0.41 M Tris-base and 2% (v/v) acetic acid.

2.6 Sample digestion

For the Homer2 co-IP experiment, proteins were digested as previously described [41]. Briefly, 25 μg of each sample was solubilized in 0.2% RapiGest buffered with 50 mM ammonium bicarbonate pH 7.8 by heating at 100 °C for 5 min followed by sonication. The samples were reduced at 60 °C for 30 min with 5 mM DTT, alkylated with 15 mM 2-iodoacetamide at room temperature for 30 min under darkness, and mixed with 1 mM $CaCl_2$. Porcine sequencing grade modified trypsin endoproteinase (Promega Corporation, Madison, WI) was added at a 1:100 enzyme to protein ratio and samples were incubated at 37 °C for 18 h. RapiGest was hydrolyzed with 120 mM hydrochloric acid, and samples were centrifuged three times 45 min at 20,000 × g to remove immiscible RapiGest by-products. The resulting digests were subjected to a peptide cleanup step using Pierce C-18 Spin Columns (Thermo Fisher Scientific, Rockford, IL) according to manufacturer's instructions. Peptides were dried using a CentriVap vacuum concentrator, suspended at 0.2 μg/μl in acidified water (0.1% v/v formic acid), and stored at -20 °C.

For the Homer2 co-IP verification experiment, the same procedure was used, but 250 ng 15N-labeled human Apolipoprotein A-I (Cambridge Isotope Labs, Inc., Tewksbury, MA) was added to a 5 ng/μl final concentration.

2.7 Nano liquid chromatography-tandem mass spectrometry (nLC-MS/MS)

For the Homer2 co-IP experiment, protein digests were analyzed by nLC-MS/MS using an EASY-nLC 1000 (Thermo Scientific, San Jose, CA) chromatography system coupled online via thermostated electrospray ionization to an Orbitrap Elite Hybrid Ion Trap-Orbitrap Mass Spectrometer (Thermo Scientific, San Jose, CA). Randomized injections of 1 μg of peptide preparations were resolved on a 75 μm id × 30 cm long fused silica analytical column (Polymicro Technologies, Phoenix, AZ) slurry-packed in-house with Aqua C18 (5 μm/125Å) stationary phase (Phenomenex, Torrance, CA). Peptides were eluted from the column at a constant flow rate of 200 nl/min using a linear 90 min gradient of 3-33% B (A = 98% water/2% ACN/0.1% formic acid; B = 99.9% ACN/0.1% formic acid). The column was heated at 40 °C to enhance the detection of hydrophobic peptides [42,43]. MS1 spectra were collected from *m/z* 400-1400 at a resolving power of 60,000 at 400 *m/z*, and precursor ion counts of 1,000,000 were acquired with a maximum injection time of 200 ms. The ten most

abundant precursor ions (excluding +1 precursor ions) were selected for fragmentation in the linear ion trap, and product ion counts of 10,000 were acquired with a maximum injection time of 100 ms. Dynamic exclusion was enabled with a repeat count of 1, and a 30 sec exclusion window and monoisotopic precursor selection was enabled.

2.8 Nano liquid chromatography-selected reaction monitoring (nLC-SRM)

For the Homer2 co-IP verification experiment, protein digests were analyzed by nLC-SRM using an EASY-nLC 1000 (Thermo Scientific, San Jose, CA) chromatography system coupled online via electrospray ionization to a TSQ Quantiva Triple Quadrupole Mass Spectrometer (Thermo Scientific, San Jose, CA). Randomized injections of 1.5 μg of peptide preparations including 15 ng of 15N-labeled human Apolipoprotein A-I were trapped using a 150 μm id × 3 cm long fused silica trapping column (Polymicro Technologies, Phoenix, AZ) slurry-packed in house with Jupiter C12 (4 μm/90Å) stationary phase (Phenomenex, Woburn, MA) then resolved on a 75 μm id × 20 cm long PicoFrit fused silica analytical column (Phenomenex, Woburn, MA) slurry-packed in-house with Aqua C18 (5 μm/125Å) stationary phase (Phenomenex, Torrance, CA). Samples were trapped with 9 μl of buffer A at 2 μl/min then peptides were eluted from the column at a constant flow rate of 200 nl/min using a linear 90 min gradient of 0-30% B (A = 94.9% water/0.1% formic acid/5% ACN; B = 4.9% water/0.1% formic acid/95% ACN). Ions were isolated in both Q1 and Q3 with resolutions of 0.7 FWHM and peptide fragmentation was performed in Q2 at 1.5 mTorr using peptide-specific collision energies. Monoisotopic +2 charge state fully-tryptic proteotypic peptides from 7 to 21 amino acids in length were monitored and data was collected using a scheduled data acquisition method with a 12 min retention time window, and a 10 ms dwell time. A static modification for cysteine carbamidomethylation (monoisotopic m/z = 57.021464) was included. Only peptides that were previously detected by nLC-MS/MS and used for MS1 full-scan filtering in the other Homer2 co-IP experiment were selected for nLC-SRM analysis. This enabled us to predict peptide elution times for scheduled data acquisition and to validate peak identity using an iRT calculator [44] that was calibrated against peptides from two external proteins: Ig gamma chain C region (UniProt identifier: P01870) and 15N-labeled human Apolipoprotein A-I. We also use a dot product similarity metric [45] to validate peak identity by comparing relative fragment ion intensities from spectral library data to SRM measurements. Only peptides with an average dot product (dotp) score ≥ 0.80 were reported (scored from 0 to 1, where 1 is the highest possible score). All SRM data acquisition methods and data analysis were performed using Skyline (daily version 3.1.1.7383) [46].

2.9 Database search pipeline

For the Homer2 co-IP experiment, peptide identifications were obtained by analyzing nLC-MS/MS data using a bioinformatic pipeline that consisted of: (1) the conversion of RAW data to compact text files using MSConvert [47], (2) the assignment of MS2 peptide features to deconvoluted MS1 peptide isotope distributions using Bullseye [48] and Hardklör [49], respectively, (3) real and decoy (randomized target database) database searches using SEQUEST (version 2.04) [50], and (4) the assignment of peptide-spectrum match false discover rate (FDR) using Percolator [51]. Triplicate biological and quadruple technical replicate injections of the input fraction and co-IP samples were searched independently and

together against a reviewed UniProt Knowledgebase/Swiss-Prot mouse proteome (07/09/2014 release, 24,679 sequences) combined with seven rabbit Ig proteins (UniProt identifiers: P01838, P01839, P01840, P01841, P01847, P01870, and P03984). An FDR threshold of 1% was used for peptide-spectrum matches. Additional search parameters included trypsin (arginine/lysine) enzyme specificity allowing for two missed cleavages, a static modification for cysteine carbamidomethylation (monoisotopic m/z = 57.021464), 10 parts per million (ppm) precursor ion mass tolerance, and 0.36 amu product ion mass tolerance. The results from the database search are included in Supplemental Table 4.

To assess if adding experimentally derived contaminants to the database altered the search results, we performed a database search with pig Trypsin (UniProt identifier: P00761), Staphylococcus aureus Immunoglobulin G-binding protein A (UniProt identifier: P38507), and 16 cutaneous human Keratin proteins (UniProt identifiers: O43790, O76009, O76011, O76013, O76013-2, O76014, O76015, P78385, P78386, Q14525, Q14532, Q14533, Q15323, Q92764, Q9NSB2, and Q9NSB4) included in the mouse proteome. The addition of these contaminants did not alter the list of significantly enriched Homer2-interacting proteins (data not shown). We also included the results of another database search including variable posttranslational modifications for methionine oxidation (monoisotopic m/z = 15.994915), asparagine/glutamine deamidation (monoisotopic m/z = 0.984016), as well as serine, threonine, and tyrosine phosphorylation (monoisotopic m/z = 79.966331) with up to two differential modifications allowed per peptide, using the database that included experimentally derived contaminants. The addition of these contaminants did not alter the list of significantly enriched Homer2-interacting proteins (data not shown). The results from the database search with variable modifications are in Supplemental Table 5.

2.10 Skyline MS1 full-scan filtering

For the Homer2 co-IP experiment, MS1 full-scan filtering was performed using Skyline (daily version 2.5.1.6157) with an approach similar to those described by Schilling *et al.* [52]. Briefly, MS1 full-scan settings were configured to count three isotope peaks (M, M+1, and M+2) for +2, +3, +4, +5, +6, and +7 precursor ions with a resolving power of 60,000 at 400 m/z for an Orbitrap mass analyzer. Retention time prediction was set to use scans within 2 min of MS/MS peptide identification events, and a background proteome was created from the same mouse/rabbit Ig proteome that was used for the database searches. The background proteome was digested with Trypsin (Arginine/Lysine|Proline) and missed cleavages were excluded. RAW data was filtered against the spectral library built with peptide search results from the database search pipeline. A structural modification for cysteine carbamidomethylation was included in the spectral library, ion match tolerance was set to 0.5 m/z, and the ten most intense product ions were filtered with an FDR cut-off score of 0.99 ($q < 0.01$) for peptides between 5 and 50 residues excluding potentially ragged ends. Repeated as well as non-proteotypic peptides were removed and all Skyline integrated peptide peaks were manually verified. Peptides that fell outside the integration boundary or had less than two peptides per protein were excluded from the analysis.

2.11 Statistical analyses

Protein level relative quantification and enrichment were performed using MSstats (daily version 2.3.5) [53-55] and implemented in RStudio (version 0.98.1102). For the Homer2 co-IP experiment, a 10-column MSstats readable file was exported from Skyline and pre-analyzed by normalizing proteins in this dataset to one rabbit Ig protein using the following four peptides: GYLPEPVTVTWNSGTLTNGVR, DTLMISR, EQQFNSTIR, and LSVPTSEWQR (Ig gamma chain C region; P01870). Pre-analysis to Ig peptides served as a loading control [56]. A model-based analysis was performed between conditions (i.e. WT versus *Homer2* KO co-IP samples) with the following settings: expanded scope of biological replication, restricted scope of technical replication, interference set to false, and equal feature variation set to true. The data was exported with positive $\log_2$ values representing enrichment in the WT versus KO co-IP samples, and proteins were deemed significantly enriched at an adjusted p-value of $q \leq 0.10$.

For the Homer2 co-IP verification experiment, the presence or absence of the Homer2-interacting proteins detected by MS1 full-scan filtering were manually verified. A protein was deemed “verified” if at least one +2 peptide used for MS1-full scan filtering was detected by SRM in anti-Homer2 IP versus anti-HA-tag IP control samples.

2.12 Data visualization

MS1 full-scan filtering and SRM data were visualized using Skyline.

3. Results and Discussion

3.1 Validation of an anti-Homer2 antibody for co-IP experiments

Alternative splicing produces multiple mammalian Homer gene products (e.g. mouse Homer1b/c, Homer2a/b, and Homer3 Isoforms 1/2) [57]. Therefore, we selected a purified anti-Homer2 antibody that recognized a conserved amino acid sequence (i.e. amino acids 121-176) specific to both murine Homer2 gene products [58]. To determine if the antibody would co-IP intact Homer2 complexes in mouse brain tissue, we performed Homer2 co-IP experiments on whole-brain post-nuclear supernatants (i.e. the input fraction for later enrichment steps) harvested from WT and *Homer2* KO mice.

It was previously reported that Homer2 proteins are posttranslationally modified [59,60]. Therefore, we used 2-D western blotting to determine if the anti-Homer2 antibody recognized and immunoprecipitated (IPed) posttranslationally modified Homer2 protein species. We observed similar spot distributions for Homer2 around 47 kDa in the input fraction and the co-IP sample, demonstrating that the antibody IPed the majority of Homer2 protein species detected in the input fraction (Figure 1B). The two bands corresponding to Homer2a and Homer2b were observed around 47 kDa and 48 kDa, which is higher than their respective predicted molecular masses of 39.5 kDa and 40.6 kDa, but consistent with posttranslational modifications adding mass and with other Homer2 western blotting data from the rat brain (e.g. [4]).

Next, we used a 1-D western blot to assess the specificity of the anti-Homer2 antibody for immunoprecipitation (IP) purposes. Homer2 was detected in the WT IP sample, but not in the KO IP sample, indicating that our antibody selectively IPed Homer2 from the mouse brain (Figure 1C, Lane 6).

Finally, we used a silver stained 1-D gel to determine if the antibody would successfully co-IP Homer2 protein complexes. We observed more extensive staining in the WT versus KO co-IP samples (Figure 1D, Lane 6), which is consistent with the enrichment of Homer2-interacting proteins in WT versus KO samples.

3.2 The majority of previously reported Homer2-interacting proteins were not identified in co-IP samples from the mouse brain

To characterize Homer2-interacting proteins in the mouse brain, we used mass spectrometry and MS1 full-scan filtering. With this approach, we detected 11 of the 31 previously reported Homer2-interacting proteins in the mouse whole-brain input fractions (Figure 2A; Figure 3A; Supplemental Data 1). Surprisingly, none of these proteins were detected in the co-IP samples, suggesting that these proteins do not interact with Homer2 in the mouse brain (Supplemental Data 1). Nonetheless, 6 of the 31 previously reported Homer2-interacting proteins were detected in the co-IP samples (Figure 2A; Figure 3A; Supplemental Data 2). We were unable to detect the remaining 14 previously reported Homer2-interacting proteins in either dataset (Figure 2A; Figure 3A).

Since we detected 11 of the 31 previously reported Homer2-interacting proteins only in the input fraction, our data argues against interactions of Homer2 with PIKE, APP751, PMCA1, PMCA4, CDC42, Drebrin, Dynamin-3, IP3R1, PLC-β-1, RhoA, and 2B28, at least in a mouse whole-brain post-nuclear supernatant. Of these 11 proteins, five were not previously reported to interact with Homer2 in mouse brain tissue (Supplemental Table 1). Using immunoprecipitation (IP) assays, APP751 [61] was shown to interact with Homer2 in HEK-293 cells while PMCA1 and PMCA4 [62] were shown to interact with Homer2 in the mouse parotid gland. APP751was also shown to interact with Homer2 *in vitro* using a human-protein microarray [63]. Moreover, Homer2 was shown to interact with RhoA [64] and 2B28 [65] in *E. coli* using ligand overlay and pull-down assays, respectively. A different set of previously reported Homer2-interacting proteins were characterized in the brain, but not in mouse brain tissue: IP and pull-down assays were used to document interactions between Homer2 and PIKE [15], PLC-β-1 [38], and Dynamin-3 [12,66] in different rat brain tissues, including the whole brain, forebrain, and cerebellum. Although we were unable to detect these proteins, it is possible that these interactions are organism-specific. Work by Salanova *et al.* demonstrated that murine Homer2 GST-fusion proteins interact with IP3R1 [67] in mouse cerebellar extracts. IP experiments performed by Shiraishi-Yamaguchi *et al.* revealed that Homer2 interacts with CDC42 [64] and Drebrin/E2 [11] in the mouse cerebellum; however, Drebrin/E2 was identified using a pan-specific Homer antibody. Results from our study suggest that Drebrin/E2 may not interact with Homer2 in the mouse brain. Interestingly, IP3R1, CDC42, and Drebrin/E2 were all previously reported to interact with Homer2 in the cerebellum, a brain region with an especially low abundance of Homer2 [19,59]. Although the cerebellum comprises approximately 12% of the mouse brain by mass

[68], the total abundance of Homer2 in complex with cerebellar proteins may be so small that it is masked in the context of a whole-brain co-IP experiment. Alternatively, our inability to detect these proteins could result from technical limitations. For example, labile or transient interactions may not be retained under our co-IP conditions.

The absence of 14 of the 31 previously reported Homer2-interacting proteins from both datasets could result from their lack of expression in the brain (Figure 2A; Figure 3A; Supplemental Table 1). Consistent with this possibility, some of these proteins are predominantly expressed outside of the brain. For example, Myo18b has been shown to develop and maintain the structure of muscle cells [69], as well as function as a tumor suppressor in human carcinomas [70,71], while the RyR1 protein functions as a calcium ion channel in the sarcoplasmic reticulum of muscle tissue [72]. Moreover, the VKORC1 protein is an essential component of the blood coagulation system [73-75]. Finally, IFT57 has been shown to modulate intraflagellar transport in photoreceptor cells [76,77]. Since we performed co-IP using mouse whole-brain post-nuclear supernatants, it is understandable that we did not detect the nuclear transport protein Importin α-P1 [78], the activated NFATc1, NFATc2, and NFATc4 transcription factor proteins (reviewed in [79]), or CSPP1, which is involved in mitotic progression, cytokinesis, and ciliogenesis [80-82]. It is also possible that other undetected proteins, which included DGL-α, eEF-2k, mGluR1-α, Rac1, and TrpC1 were not detected due to their physical properties or because additional enrichment strategies were not employed. DGL-α, mGluR1-α, and TrpC1 are integral membrane proteins, which are notoriously difficult types of proteins to detect by traditional shotgun proteomics approaches [83]; moreover, unlike the highly abundant mGluR5 protein, an integral membrane protein and previously reported Homer2-interacting protein [4,5,12,13,38,84,85] that was detected in the input fraction, global mGluR1-α expression is much lower, at least in the rat brain [86]. A search of the PeptideAtlas compendium (build: Mouse 2016-01) [87,88] revealed that eEF-2k, Rac1, and TrpC1 proteins were detected by mass spectrometry in mouse brain fractions or neural cell lines, which could indicate that our protein solubilization procedure was too mild to solubilize these proteins. Interestingly, we previously detected peptides corresponding to DGL-α and mGluR1-α in mouse brain tissue, but after an enrichment for PSD proteins [89].

Overall, these data indicate that interactions between Homer2 and a subset of previously reported Homer2-interacting proteins might be organism-, cell line-, or even tissue-specific.

3.3 Enrichment analysis identifies novel Homer2-interacting proteins in the mouse brain

MS1 full-scan filtering enabled us to measure relative quantitative differences in protein abundance between samples that do not share identical peptide identification events [89]. Accordingly, we used this method to detect Homer2-interacting proteins that were enriched in WT versus *Homer2* KO co-IP samples.

Altogether, 144 proteins were detected by MS1 full-scan filtering in WT and *Homer2* KO co-IP samples (Supplemental Table 2, Tab 1). After checking the CRAPome (database version 1.1), a repository for contaminants commonly identified in mass spectrometry-based co-IP experiments [90], we flagged and discarded co-IP proteins that were identified more than 50 times. This resulted in the removal of half (72) of the proteins from the dataset

(Supplemental Table 2, Tab 2). Even though this strategy runs the risk of excluding truly interacting proteins, like β-actin, a previously reported Homer2-interacting protein [64], this strategy reduces the potential for false positives.

Next, we assessed protein enrichment by comparing the remaining 72 proteins between WT and *Homer2* KO co-IP samples. At a 10% false discovery rate (FDR), a less stringent cutoff value facilitating the validation of more proteins by SRM, 22 proteins were significantly enriched in WT co-IP samples, including four previously reported Homer2-interacting proteins (Figure 2B; Figure 3B; Supplemental Table 2, Tab 3). Furthermore, we were able to detect 19 of the 22 significantly enriched proteins using SRM in a second Homer2 co-IP verification experiment (Figure 3B; Supplemental Figure 1; Supplemental Data 3). Together, these data indicate that in the mouse brain Homer2 proteins mostly interact with a different subset of proteins than those previously reported in the literature.

The results of our Homer2 co-IP experiments are consistent with the molecular properties of Homer2 proteins, namely their ability to bind specific proline-rich motifs (e.g. PPXXF and PXXF where X is any amino acid) found in several proteins [6,12-15] and to multimerize with longer (constitutively expressed) Homer proteins [4,5,7-11]. The majority of the proteins contained at least one proline-rich Homer binding motif (Supplemental Table 2, Tab 3). This includes Shank3, a previously reported Homer2-interacting protein with the PPXXF motif [13]. Out of the 19 SRM-verified proteins, only four proteins that were significantly enriched in WT samples did not contain a proline-rich motif. These proteins were: BAIAP2, CaMKII-α, CaMKII-β, and ZC2HC1A. Each of these four proteins interacts with other significantly enriched proteins that have a proline-rich binding motif, suggesting that they are second-order interactors (Figure 4). In stark contrast, a majority of the unenriched proteins that lack a Homer binding motif do not interact with proteins containing a Homer binding motif or collectively form a signaling pathway. Two notable exceptions were: CaMKII-δ and CaMKII-γ because both of these proteins likely form heteromultimeric holoenzymes with the significantly enriched CaMKII-α and CaMKII-β proteins [91]. Interestingly, neither significantly enriched nor unenriched proteins contained the LPSSP motif despite its presence in five previously reported Homer2-interacting proteins, including: PIKE [15], eEF-2k [17], Myo18b [71], NFATc4 [84], and TrpC1 [16]. Moreover, all three proteins that were not verified by SRM only contained the PXXF motif (Supplemental Table 2, Tab 3). Thus, the fact that none of the verified interactors of Homer2 contained the LPSSP or PXXF motifs suggest that Homer2 protein binding interactions favor the PPXXF motif.

Homer1 and Homer3 were also significantly enriched in WT co-IP samples (Figure 3B; Supplemental Table 2, Tab 3). We believe this observation confirms that longer (constitutively expressed) Homer proteins multimerize with Homer2 through their carboxyl-terminal coiled-coil domains, although it is possible that Homer1 and Homer3 co-IP with Homer2 indirectly though one or more undetermined mutual interacting proteins. This is the first time interactions between Homer2, Homer1, and Homer3 were found in mouse brain tissue. Previous experiments documenting Homer2 homomultimerization and heteromultimerization used fusion proteins expressed in *E.coli* [4,5,11], and an attempt to co-IP Homer2 using anti-Homer1b/c and anti-Homer3 antibodies did not succeed in rat brain cerebellar extracts [4] (probably because of the low abundance of Homer2 in the

cerebellum). More recently, an affinity purification based mass spectrometry experiment found an interaction between Homer2 and Homer1, but this was documented in HEK-293 cells [92]. Furthermore, the significant enrichment of Homer1 and Homer3 confirms the specificity of the anti-Homer2 antibody used in our co-IP experiments; if antibody cross-reactivity had occurred, Homer1 and Homer3 proteins would not be significantly enriched in WT versus KO co-IP samples.

These results are also consistent with the subcellular localization of Homer2 proteins at the PSD. An elegant study by Tao-Cheng *et al.* demonstrated by electron microscopy that Homer2 is evenly distributed along the lateral axis directly below the PSD core in the mouse cerebral cortex and rat dissociated hippocampal cultures [19]. Coupled with observations that some previously reported Homer2-interacting proteins are located outside of the PSD core, specifically Group I mGluRs (i.e. mGluR1-α and mGluR5) (reviewed in [93]), and IP3Rs (except in the cerebellum [94]), the authors hypothesized that spatial proximity could limit interactions between Homer proteins and their interacting partners. In other words, proteins must be very close to interact with each other. Our data support this hypothesis since mGluR1-α, mGluR5, and IP3R1 were not enriched in WT co-IP samples, but Shank proteins, which share the same space as Homer2 in the PSD core [10,19,95], were enriched in WT samples (Figure 3B; Supplemental Table 2, Tab 3). Moreover, different electron microscopy experiments revealed that PSD structure is retained after detergent solubilization in a buffer similar to our co-IP buffer (i.e. 1% Triton X-100) [96,97], and a comparative analysis of data collected from several proteomics studies proposed that the PSD contains approximately 466 “consensus” proteins [98]. Since we only detected 72 proteins (excluding contaminants) in our co-IP samples after MS1 full-scan filtering (Supplemental Table 2, Tabs 3/4), these data indicate that we co-IPed specific Homer2-interacting proteins, not the entire PSD.

Furthermore, the overlap between the Homer2-interacting proteins and recent proteomic characterizations of the PSD suggests that most of the Homer2-interacting proteins we detected are components of the PSD. Only three (i.e. RhoGEF33, PITRM1, and ZC2HC1A) of the 18 Homer2-interacting proteins we verified were not in the “high-confidence PSD dataset” reported by Distler *et al.* [99]. Additionally, six (RhoGEF33, PITRM1, and ZC2HC1A as well as Homer3, LRRC7, and PITRM1) of the 18 Homer2-interacting proteins were not found in the data acquired by Föcking *et al.* [100]. We co-immunoprecipitated from whole brain post-nuclear supernatants, but Distler *et al.* and Föcking *et al.* examined the mouse hippocampus and human anterior cingulate cortex, respectively. So, the different overlap between our data and theirs could be attributed to brain region specific PSD proteins.

Altogether, our data provide novel insight into the function of Homer2 in the mouse brain, as the majority of the interactors we identified are part of the NMDAR signaling pathway. These include two NMDAR subunits: GluN1 and GluN2B. Interestingly, both proteins have proline-rich Homer binding motifs (Supplemental Table 2, Tab 3), which suggests that GluN1 and GluN2B co-IP with Homer2 through direct protein-protein interactions. We also detected four proteins that indirectly link NMDARs to the actin cytoskeleton: PSD-95, Shank1, Shank2, and Shank3 [13,101]. Theoretically, these interactions could mediate the

trafficking of NMDAR subunits to the plasma membrane. They could also further establish a link between Homer2 proteins, NMDAR signaling events, and alcohol addiction (reviewed in [31,32]).

Most notably, and consistent with the hypothesis that NMDAR activation initiates cellular learning and memory mechanism that could reinforce the rewarding effects of alcohol consumption, two key proteins involved in NMDAR-mediated long-term potentiation (LTP) were significantly enriched in WT samples: CaMKII-α and CaMKII-β [102]. While these proteins do not contain any proline-rich Homer binding motifs, they were reported to interact with NMDAR subunits [102] and other co-IPed proteins (Supplemental Table 3), including: LRRC7, ANKS1B, and SYNGAP1. Interestingly, CaMKII-α activity, specifically CaMKII-α autophosphorylation, was shown to modulate the development of alcohol-induced conditioned place preference in mice [103]. Consistent with this observation, single nucleotide polymorphisms (SNPs) in the *Camk2a* gene have been associated with alcohol dependence, and one of these SNPs was observed in an area of the gene related to autophosphorylation [103].

Furthermore, our Homer2 co-IP experiments identified three Homer2-interacting proteins without any known NMDAR affiliation. These proteins were: PITRM1, RhoGEF33, and ZC2HC1A. A literature review did not reveal any previously reported association with Homer2 proteins, but an SNP was reported in the human *Pitrm1* gene in a genome-wide association study of alcohol dependence [104].

4. Conclusions

Previous studies identified 31 interaction partners of Homer2 in a wide variety of organisms, tissues, and cell lines. However, the results of our Homer2 co-IP experiments in mouse whole-brain tissue revealed a different list of interactors: of the 31 previously reported Homer2-interacting proteins, 11 proteins were only detected in the input fractions used for co-IP, 6 proteins were detected in the co-IP samples, and 14 proteins were not detected in either sample set. Strikingly, only 3 of the 6 previously reported Homer2-interacting proteins detected in co-IP samples were significantly enriched in WT versus KO samples (this excludes Homer2 because our co-IP experiments cannot differentiate Homer2 proteins directly bound by the antibody from Homer2 homomultimers). However, we detected 18 additional “novel” Homer2-interacting proteins. Since we were unable to verify 3 of these proteins by SRM using a different cohort of mice, we only report 18 proteins as high-confidence Homer2-interacting proteins in the mouse brain (Figure 4). The majority of these 18 proteins participate in NMDAR signal transduction, which further implicates the Homer2 protein in signaling events that mediate glutamatergic transmission and synaptic plasticity.

Supplementary Material

Refer to Web version on PubMed Central for supplementary material.

Acknowledgments

This work was supported by NIH grants T32 HD041697 and T32 AA007456 to SPG, R01 DA024038 and R01 AA016650 to KKS, U01 AA020913 and R21 AA024198 to CC, P41 GM103533 to MJM, and R01 AA016171, U01 AA016653, and S10 RR027928 to CCW. We would like to thank Dr. John H. Caldwell for critiquing experiments in this manuscript, Dr. Nicholas W. Bateman, Dr. James G. Bollinger, and Gennifer Merrihew for technical assistance, Nicholas J. Shulman, Han-Yin Yang, Dr. Ying Ting, and especially Dr. Jarrett D. Egertson for their computational help. We would also like to thank the laboratory of Dr. Paul F. Worley (Department of Neuroscience, Johns Hopkins University School of Medicine) for originally supplying the Szumlinski laboratory with *Homer2* heterozygotes upon which the current mouse colonies are based.

References

1. Shiraishi-Yamaguchi Y, Furuichi T. The Homer family proteins. Genome Biol. 2007; 8:206.doi: 10.1186/gb-2007-8-2-206 [PubMed: 17316461]
2. Kato A, Ozawa F, Saitoh Y, Hirai K, Inokuchi K. vesl, a gene encoding VASP/Ena family related protein, is upregulated during seizure, long-term potentiation and synaptogenesis. FEBS Lett. 1997; 412:183–189. [PubMed: 9257717]
3. Brakeman PR, Lanahan AA, O'Brien R, Roche K, Barnes CA, Huganir RL, et al. Homer: a protein that selectively binds metabotropic glutamate receptors. Nature. 1997; 386:284.doi: 10.1038/386284a0 [PubMed: 9069287]
4. Xiao B, Tu JC, Petralia RS, Yuan JP, Doan A, Breder CD, et al. Homer regulates the association of group 1 metabotropic glutamate receptors with multivalent complexes of homer-related, synaptic proteins. Neuron. 1998; 21:707–716. [PubMed: 9808458]
5. Kato A, Ozawa F, Saitoh Y, Fukazawa Y, Sugiyama H, Inokuchi K. Novel members of the Vesl/Homer family of PDZ proteins that bind metabotropic glutamate receptors. J Biol Chem. 1998; 273:23969–23975. [PubMed: 9727012]
6. Barzik M, Carl UD, Schubert WD, Frank R, Wehland J, Heinz DW. The N-terminal domain of Homer/Vesl is a new class II EVH1 domain. J Mol Biol. 2001; 309:155–169. DOI: 10.1006/jmbi.2001.4640 [PubMed: 11491285]
7. Sun J, Tadokoro S, Imanaka T, Murakami SD, Nakamura M, Kashiwada K, et al. Isolation of PSD-Zip45, a novel Homer/vesl family protein containing leucine zipper motifs, from rat brain. FEBS Lett. 1998; 437:304–308. [PubMed: 9824313]
8. Tadokoro S, Tachibana T, Imanaka T, Nishida W, Sobue K. Involvement of unique leucine-zipper motif of PSD-Zip45 (Homer 1c/vesl-1L) in group 1 metabotropic glutamate receptor clustering. Proc Natl Acad Sci USA. 1999; 96:13801–13806. [PubMed: 10570153]
9. Hayashi MK, Ames HM, Hayashi Y. Tetrameric hub structure of postsynaptic scaffolding protein homer. J Neurosci. 2006; 26:8492–8501. DOI: 10.1523/JNEUROSCI.2731-06.2006 [PubMed: 16914674]
10. Hayashi MK, Tang C, Verpelli C, Narayanan R, Stearns MH, Xu RM, et al. The postsynaptic density proteins Homer and Shank form a polymeric network structure. Cell. 2009; 137:159–171. DOI: 10.1016/j.cell.2009.01.050 [PubMed: 19345194]
11. Shiraishi-Yamaguchi Y, Sato Y, Sakai R, Mizutani A, Knöpfel T, Mori N, et al. Interaction of Cupidin/Homer2 with two actin cytoskeletal regulators, Cdc42 small GTPase and Drebrin, in dendritic spines. BMC Neurosci. 2009; 10:25.doi: 10.1186/1471-2202-10-25 [PubMed: 19309525]
12. Tu JC, Xiao B, Yuan JP, Lanahan AA, Leoffert K, Li M, et al. Homer binds a novel proline-rich motif and links group 1 metabotropic glutamate receptors with IP3 receptors. Neuron. 1998; 21:717–726. [PubMed: 9808459]
13. Tu JC, Xiao B, Naisbitt S, Yuan JP, Petralia RS, Brakeman P, et al. Coupling of mGluR/Homer and PSD-95 complexes by the Shank family of postsynaptic density proteins. Neuron. 1999; 23:583–592. [PubMed: 10433269]
14. Beneken J, Tu JC, Xiao B, Nuriya M, Yuan JP, Worley PF, et al. Structure of the Homer EVH1 domain-peptide complex reveals a new twist in polyproline recognition. Neuron. 2000; 26:143–154. [PubMed: 10798399]

15. Rong R, Ahn JY, Huang H, Nagata E, Kalman D, Kapp JA, et al. PI3 kinase enhancer-Homer complex couples mGluRI to PI3 kinase, preventing neuronal apoptosis. Nat Neurosci. 2003; 6:1153–1161. DOI: 10.1038/nn1134 [PubMed: 14528310]

16. Yuan JP, Kiselyov K, Shin DM, Chen J, Shcheynikov N, Kang SH, et al. Homer binds TRPC family channels and is required for gating of TRPC1 by IP3 receptors. Cell. 2003; 114:777–789. [PubMed: 14505576]

17. Park S, Park JM, Kim S, Kim JA, Shepherd JD, Smith-Hicks CL, et al. Elongation factor 2 and fragile X mental retardation protein control the dynamic translation of Arc/Arg3.1 essential for mGluR-LTD. Neuron. 2008; 59:70–83. DOI: 10.1016/j.neuron.2008.05.023 [PubMed: 18614030]

18. Shiraishi Y, Mizutani A, Yuasa S, Mikoshiba K, Furuichi T. Differential expression of Homer family proteins in the developing mouse brain. The Journal of Comparative Neurology. 2004; 473:582–599. DOI: 10.1002/cne.20116 [PubMed: 15116392]

19. Tao-Cheng JH, Thein S, Yang Y, Reese TS, Gallant PE. Homer is concentrated at the postsynaptic density and does not redistribute after acute synaptic stimulation. Neuroscience. 2014; 266:80–90. DOI: 10.1016/j.neuroscience.2014.01.066 [PubMed: 24530450]

20. Berke JD, Paletzki RF, Aronson GJ, Hyman SE, Gerfen CR. A complex program of striatal gene expression induced by dopaminergic stimulation. J Neurosci. 1998; 18:5301–5310. [PubMed: 9651213]

21. Sala C, Piëch V, Wilson NR, Passafaro M, Liu G, Sheng M. Regulation of dendritic spine morphology and synaptic function by Shank and Homer. Neuron. 2001; 31:115–130. [PubMed: 11498055]

22. Sala C, Futai K, Yamamoto K, Worley PF, Hayashi Y, Sheng M. Inhibition of dendritic spine morphogenesis and synaptic transmission by activity-inducible protein Homer1a. J Neurosci. 2003; 23:6327–6337. [PubMed: 12867517]

23. Meyer D, Bonhoeffer T, Scheuss V. Balance and stability of synaptic structures during synaptic plasticity. Neuron. 2014; 82:430–443. DOI: 10.1016/j.neuron.2014.02.031 [PubMed: 24742464]

24. McGuier NS, Padula AE, Mulholland PJ, Chandler LJ. Homer2 deletion alters dendritic spine morphology but not alcohol-associated adaptations in GluN2B-containing N-methyl-D-aspartate receptors in the nucleus accumbens. Front Pharmacol. 2015; 6:28.doi: 10.3389/fphar.2015.00028 [PubMed: 25755642]

25. de Bartolomeis A, Iasevoli F. The Homer family and the signal transduction system at glutamatergic postsynaptic density: potential role in behavior and pharmacotherapy. Psychopharmacology Bulletin. 2003; 37:51–83. [PubMed: 14608240]

26. Obara I, Goulding SP, Gould AT, Lominac KD, Hu JH, Zhang PW, et al. Homers at the Interface between Reward and Pain. Front Psychiatry. 2013; 4:39.doi: 10.3389/fpsyt.2013.00039 [PubMed: 23761764]

27. Szumlinski KK, Lominac KD, Kleschen MJ, Oleson EB, Dehoff MH, Schwartz MK, et al. Behavioral and neurochemical phenotyping of Homer1 mutant mice: possible relevance to schizophrenia. Genes, Brain, and Behavior. 2005; 4:273–288. DOI: 10.1111/j.1601-183X.2005.00120.x

28. Szumlinski KK, Dehoff MH, Kang SH, Frys KA, Lominac KD, Klugmann M, et al. Homer proteins regulate sensitivity to cocaine. Neuron. 2004; 43:401–413. DOI: 10.1016/j.neuron.2004.07.019 [PubMed: 15294147]

29. Szumlinski KK, Abernathy KE, Oleson EB, Klugmann M, Lominac KD, He DY, et al. Homer isoforms differentially regulate cocaine-induced neuroplasticity. Neuropsychopharmacology. 2006; 31:768–777. DOI: 10.1038/sj.npp.1300890 [PubMed: 16160706]

30. Ary AW, Lominac KD, Wroten MG, Williams AR, Campbell RR, Ben-Shahar O, et al. Imbalances in Prefrontal Cortex CC-Homer1 versus CC-Homer2 Expression Promote Cocaine Preference. J Neurosci. 2013; 33:8101–8113. DOI: 10.1523/JNEUROSCI.1727-12.2013 [PubMed: 23658151]

31. Szumlinski KK, Kalivas PW, Worley PF. Homer proteins: implications for neuropsychiatric disorders. Curr Opin Neurobiol. 2006; 16:251–257. DOI: 10.1016/j.conb.2006.05.002 [PubMed: 16704932]

32. Szumlinski KK, Ary AW, Lominac KD. Homers regulate drug-induced neuroplasticity: implications for addiction. Biochem Pharmacol. 2008; 75:112–133. DOI: 10.1016/j.bcp.2007.07.031 [PubMed: 17765204]
33. Szumlinski KK, Lominac KD, Oleson EB, Walker JK, Mason A, Dehoff MH, et al. Homer2 is necessary for EtOH-induced neuroplasticity. J Neurosci. 2005; 25:7054–7061. DOI: 10.1523/JNEUROSCI.1529-05.2005 [PubMed: 16049182]
34. Szumlinski KK, Ary AW, Lominac KD, Klugmann M, Kippin TE. Accumbens Homer2 overexpression facilitates alcohol-induced neuroplasticity in C57BL/6J mice. Neuropsychopharmacology. 2008; 33:1365–1378. DOI: 10.1038/sj.npp.1301473 [PubMed: 17568396]
35. Cozzoli DK, Goulding SP, Zhang PW, Xiao B, Hu JH, Ary AW, et al. Binge drinking upregulates accumbens mGluR5-Homer2-PI3K signaling: functional implications for alcoholism. J Neurosci. 2009; 29:8655–8668. DOI: 10.1523/JNEUROSCI.5900-08.2009 [PubMed: 19587272]
36. Goulding SP, Obara I, Lominac KD, Gould AT, Miller BW, Klugmann M, et al. Accumbens Homer2-mediated signaling: a factor contributing to mouse strain differences in alcohol drinking? Genes, Brain, and Behavior. 2011; 10:111–126. DOI: 10.1111/j.1601-183X.2010.00647.x
37. Ary AW, Cozzoli DK, Finn DA, Crabbe JC, Dehoff MH, Worley PF, et al. Ethanol up-regulates nucleus accumbens neuronal activity dependent pentraxin (Narp): implications for alcohol-induced behavioral plasticity. Alcohol. 2012; 46:377–387. DOI: 10.1016/j.alcohol.2011.10.003 [PubMed: 22444953]
38. Shin DM. Homer 2 tunes G protein-coupled receptors stimulus intensity by regulating RGS proteins and PLC GAP activities. J Cell Biol. 2003; 162:293–303. DOI: 10.1083/jcb.200210109 [PubMed: 12860966]
39. Wessel D, Flügge UI. A method for the quantitative recovery of protein in dilute solution in the presence of detergents and lipids. Anal Biochem. 1984; 138:141–143. [PubMed: 6731838]
40. Wu CC, Taylor RS, Lane DR, Ladinsky MS, Weisz JA, Howell KE. GMx33: A Novel Family of trans-Golgi Proteins Identified by Proteomics. Traffic. 2008; 1:963–975. DOI: 10.1111/j.1600-0854.2000.11206.x
41. Goulding SP, MacCoss MJ, Wu CC. Label-free differential analysis of murine postsynaptic densities. Methods Mol Biol. 2013; 1002:295–309. DOI: 10.1007/978-1-62703-360-2_22 [PubMed: 23625411]
42. Speers AE, Wu CC. Proteomics of integral membrane proteins--theory and application. Chem Rev. 2007; 107:3687–3714. DOI: 10.1021/cr068286z [PubMed: 17683161]
43. Farias SE, Kline KG, Klepacki J, Wu CC. Quantitative improvements in peptide recovery at elevated chromatographic temperatures from microcapillary liquid chromatography-mass spectrometry analyses of brain using selected reaction monitoring. Anal Chem. 2010; 82:3435–3440. DOI: 10.1021/ac100359p [PubMed: 20373813]
44. Escher C, Reiter L, MacLean B, Ossola R, Herzog F, Chilton J, et al. Using iRT, a normalized retention time for more targeted measurement of peptides. Proteomics. 2012; 12:1111–1121. DOI: 10.1002/pmic.201100463 [PubMed: 22577012]
45. Tabb DL, MacCoss MJ, Wu CC, Anderson SD, Yates JR. Similarity among tandem mass spectra from proteomic experiments: detection, significance, and utility. Anal Chem. 2003; 75:2470–2477. DOI: 10.1021/ac026424o [PubMed: 12918992]
46. MacLean B, Tomazela DM, Abbatiello SE, Zhang S, Whiteaker JR, Paulovich AG, et al. Effect of collision energy optimization on the measurement of peptides by selected reaction monitoring (SRM) mass spectrometry. Anal Chem. 2010; 82:10116–10124. DOI: 10.1021/ac102179j [PubMed: 21090646]
47. Chambers MC, MacLean B, Burke R, Amodei D, Ruderman DL, Neumann S, et al. A cross-platform toolkit for mass spectrometry and proteomics. Nat Biotechnol. 2012; 30:918–920. DOI: 10.1038/nbt.2377 [PubMed: 23051804]
48. Hsieh EJ, Hoopmann MR, MacLean B, MacCoss MJ. Comparison of database search strategies for high precursor mass accuracy MS/MS data. J Proteome Res. 2010; 9:1138–1143. DOI: 10.1021/pr900816a [PubMed: 19938873]

49. Hoopmann MR, Finney GL, MacCoss MJ. High-speed data reduction, feature detection, and MS/MS spectrum quality assessment of shotgun proteomics data sets using high-resolution mass spectrometry. Anal Chem. 2007; 79:5620–5632. DOI: 10.1021/ac0700833 [PubMed: 17580982]
50. Eng JK, McCormack AL, Yates JR. An approach to correlate tandem mass spectral data of peptides with amino acid sequences in a protein database. J Am Soc Mass Spectrom. 1994; 5:976–989. DOI: 10.1016/1044-0305(94)80016-2 [PubMed: 24226387]
51. Käll L, Storey JD, MacCoss MJ, Noble WS. Assigning significance to peptides identified by tandem mass spectrometry using decoy databases. J Proteome Res. 2008; 7:29–34. DOI: 10.1021/pr700600n [PubMed: 18067246]
52. Schilling B, Rardin MJ, MacLean BX, Zawadzka AM, Frewen BE, Cusack MP, et al. Platform-independent and label-free quantitation of proteomic data using MS1 extracted ion chromatograms in skyline: application to protein acetylation and phosphorylation. Molecular & Cellular Proteomics. 2012; 11:202–214. DOI: 10.1074/mcp.M112.017707 [PubMed: 22454539]
53. Chang CY, Picotti P, Huttenhain R, Heinzelmann-Schwarz V, Jovanovic M, Aebersold R, et al. Protein Significance Analysis in Selected Reaction Monitoring (SRM) Measurements. Molecular & Cellular Proteomics. 2012; 11:M111.014662–M111.014662. DOI: 10.1074/mcp.M111.014662
54. Clough T, Thaminy S, Ragg S, Aebersold R, Vitek O. Statistical protein quantification and significance analysis in label-free LC-MS experiments with complex designs. BMC Bioinformatics. 2012; 13(Suppl 16):S6.doi: 10.1186/1471-2105-13-S16-S6
55. Weisser H, Nahnsen S, Grossmann J, Nilse L, Quandt A, Brauer H, et al. An automated pipeline for high-throughput label-free quantitative proteomics. J Proteome Res. 2013; 12:1628–1644. DOI: 10.1021/pr300992u [PubMed: 23391308]
56. Rogstad SM, Sorkina T, Sorkin A, Wu CC. Improved precision of proteomic measurements in immunoprecipitation based purifications using relative quantitation. Anal Chem. 2013; 85:4301–4306. DOI: 10.1021/ac4002222 [PubMed: 23517085]
57. Bottai D, Guzowski JF, Schwarz MK, Kang SH, Xiao B, Lanahan A, et al. Synaptic activity-induced conversion of intronic to exonic sequence in Homer 1 immediate early gene expression. J Neurosci. 2002; 22:167–175. [PubMed: 11756499]
58. Soloviev MM, Ciruela F, Chan WY, McIlhinney RA. Molecular characterisation of two structurally distinct groups of human homers, generated by extensive alternative splicing. J Mol Biol. 2000; 295:1185–1200. DOI: 10.1006/jmbi.1999.3436 [PubMed: 10653696]
59. Shiraishi Y, Mizutani A, Mikoshiba K, Furuichi T. Coincidence in dendritic clustering and synaptic targeting of homer proteins and NMDA receptor complex proteins NR2B and PSD95 during development of cultured hippocampal neurons. Molecular and Cellular Neuroscience. 2003; 22:188–201. DOI: 10.1016/S1044-7431(03)00037-X [PubMed: 12676529]
60. Shiraishi Y, Mizutani A, Yuasa S, Mikoshiba K, Furuichi T. Glutamate-induced declustering of post-synaptic adaptor protein Cupidin (Homer 2/vesl-2) in cultured cerebellar granule cells. J Neurochem. 2003; 87:364–376. [PubMed: 14511114]
61. Parisiadou L, Bethani I, Michaki V, Krousti K, Rapti G, Efthimiopoulos S. Homer2 and Homer3 interact with amyloid precursor protein and inhibit Abeta production. Neurobiol Dis. 2008; 30:353–364. DOI: 10.1016/j.nbd.2008.02.004 [PubMed: 18387811]
62. Yang YM, Lee J, Jo H, Park S, Chang I, Muallem S, et al. Homer2 protein regulates plasma membrane Ca^{2+}-ATPase-mediated Ca^{2+} signaling in mouse parotid gland acinar cells. Journal of Biological Chemistry. 2014; 289:24971–24979. DOI: 10.1074/jbc.M114.577221 [PubMed: 25049230]
63. Olah J, Vincze O, Virok D, Simon D, Bozso Z, Tokesi N, et al. Interactions of Pathological Hallmark Proteins: TUBULIN POLYMERIZATION PROMOTING PROTEIN/p25, -AMYLOID, AND -SYNUCLEIN. Journal of Biological Chemistry. 2011; 286:34088–34100. DOI: 10.1074/jbc.M111.243907 [PubMed: 21832049]
64. Shiraishi Y, Mizutani A, Bito H, Fujisawa K, Narumiya S, Mikoshiba K, et al. Cupidin, an isoform of Homer/Vesl, interacts with the actin cytoskeleton and activated rho family small GTPases and is expressed in developing mouse cerebellar granule cells. J Neurosci. 1999; 19:8389–8400. [PubMed: 10493740]

65. Ishibashi T, Ogawa S, Hashiguchi Y, Inoue Y, Udo H, Ohzono H, et al. A novel protein specifically interacting with Homer2 regulates ubiquitin-proteasome systems. J Biochem. 2005; 137:617–623. DOI: 10.1093/jb/mvi074 [PubMed: 15944415]
66. Gray NW, Fourgeaud L, Huang B, Chen J, Cao H, Oswald BJ, et al. Dynamin 3 is a component of the postsynapse, where it interacts with mGluR5 and Homer. Curr Biol. 2003; 13:510–515. [PubMed: 12646135]
67. Salanova M, Priori G, Barone V, Intravaia E, Flucher B, Ciruela F, et al. Homer proteins and InsP(3) receptors co-localise in the longitudinal sarcoplasmic reticulum of skeletal muscle fibres. Cell Calcium. 2002; 32:193–200. [PubMed: 12379179]
68. Airey DC, Lu L, Williams RW. Genetic control of the mouse cerebellum: identification of quantitative trait loci modulating size and architecture. J Neurosci. 2001; 21:5099–5109. [PubMed: 11438585]
69. Ajima R, Akazawa H, Kodama M, Takeshita F, Otsuka A, Kohno T, et al. Deficiency of Myo18B in mice results in embryonic lethality with cardiac myofibrillar aberrations. Genes Cells. 2008; 13:987–999. DOI: 10.1111/j.1365-2443.2008.01226.x [PubMed: 18761673]
70. Nishioka M, Kohno T, Tani M, Yanaihara N, Tomizawa Y, Otsuka A, et al. MYO18B, a candidate tumor suppressor gene at chromosome 22q12.1, deleted, mutated, and methylated in human lung cancer. Proc Natl Acad Sci USA. 2002; 99:12269–12274. DOI: 10.1073/pnas.192445899 [PubMed: 12209013]
71. Ajima R, Kajiya K, Inoue T, Tani M, Shiraishi-Yamaguchi Y, Maeda M, et al. HOMER2 binds MYO18B and enhances its activity to suppress anchorage independent growth. Biochem Biophys Res Commun. 2007; 356:851–856. DOI: 10.1016/j.bbrc.2007.03.060 [PubMed: 17386922]
72. Giannini G, Conti A, Mammarella S, Scrobogna M, Sorrentino V. The ryanodine receptor/calcium channel genes are widely and differentially expressed in murine brain and peripheral tissues. J Cell Biol. 1995; 128:893–904. [PubMed: 7876312]
73. Rost S, Fregin A, Ivaskevicius V, Conzelmann E, Hörtnagel K, Pelz HJ, et al. Mutations in VKORC1 cause warfarin resistance and multiple coagulation factor deficiency type 2. Nature. 2004; 427:537–541. DOI: 10.1038/nature02214 [PubMed: 14765194]
74. Schaafhausen A, Rost S, Oldenburg J, Müller CR. Identification of VKORC1 interaction partners by split-ubiquitin system and coimmunoprecipitation. Thromb Haemost. 2011; 105:285–294. DOI: 10.1160/TH10-07-0483 [PubMed: 21103663]
75. Hammed A, Matagrin B, Spohn G, Prouillac C, Benoit E, Lattard V. VKORC1L1, an enzyme rescuing the vitamin K 2,3-epoxide reductase activity in some extrahepatic tissues during anticoagulation therapy. Journal of Biological Chemistry. 2013; 288:28733–28742. DOI: 10.1074/jbc.M113.457119 [PubMed: 23928358]
76. Krock BL, Perkins BD. The intraflagellar transport protein IFT57 is required for cilia maintenance and regulates IFT-particle-kinesin-II dissociation in vertebrate photoreceptors. J Cell Sci. 2008; 121:1907–1915. DOI: 10.1242/jcs.029397 [PubMed: 18492793]
77. Sukumaran S, Perkins BD. Early defects in photoreceptor outer segment morphogenesis in zebrafish ift57, ift88 and ift172 Intraflagellar Transport mutants. Vision Res. 2009; 49:479–489. DOI: 10.1016/j.visres.2008.12.009 [PubMed: 19136023]
78. Fontes MRM, Teh T, Jans D, Brinkworth RI, Kobe B. Structural basis for the specificity of bipartite nuclear localization sequence binding by importin-alpha. J Biol Chem. 2003; 278:27981–27987. DOI: 10.1074/jbc.M303275200 [PubMed: 12695505]
79. Rao A, Luo C, Hogan PG. Transcription factors of the NFAT family: regulation and function. Annu Rev Immunol. 1997; 15:707–747. DOI: 10.1146/annurev.immunol.15.1.707 [PubMed: 9143705]
80. Patzke S, Stokke T, Aasheim HC. CSPP and CSPP-L associate with centrosomes and microtubules and differently affect microtubule organization. J Cell Physiol. 2006; 209:199–210. DOI: 10.1002/jcp.20725 [PubMed: 16826565]
81. Asiedu M, Wu D, Matsumura F, Wei Q. Centrosome/spindle pole-associated protein regulates cytokinesis via promoting the recruitment of MyoGEF to the central spindle. Molecular Biology of the Cell. 2009; 20:1428–1440. DOI: 10.1091/mbc.E08-01-0001 [PubMed: 19129481]

82. Patzke S, Redick S, Warsame A, Murga-Zamalloa CA, Khanna H, Doxsey S, et al. CSPP is a ciliary protein interacting with Nephrocystin 8 and required for cilia formation. Molecular Biology of the Cell. 2010; 21:2555–2567. DOI: 10.1091/mbc.E09-06-0503 [PubMed: 20519441]
83. Wu CC, MacCoss MJ, Howell KE, Yates JR. A method for the comprehensive proteomic analysis of membrane proteins. Nat Biotechnol. 2003; 21:532–538. DOI: 10.1038/nbt819 [PubMed: 12692561]
84. Huang GN, Huso DL, Bouyain S, Tu J, McCorkell KA, May MJ, et al. NFAT binding and regulation of T cell activation by the cytoplasmic scaffolding Homer proteins. Science. 2008; 319:476–481. DOI: 10.1126/science.1151227 [PubMed: 18218901]
85. Loweth JA, Scheyer AF, Milovanovic M, LaCrosse AL, Flores-Barrera E, Werner CT, et al. Synaptic depression via mGluR1 positive allosteric modulation suppresses cue-induced cocaine craving. Nature Publishing Group. 2014; 17:73–80. DOI: 10.1038/nn.3590
86. Ferraguti F, Shigemoto R. Metabotropic glutamate receptors. Cell Tissue Res. 2006; 326:483–504. DOI: 10.1007/s00441-006-0266-5 [PubMed: 16847639]
87. Desiere F, Deutsch EW, Nesvizhskii AI, Mallick P, King NL, Eng JK, et al. Integration with the human genome of peptide sequences obtained by high-throughput mass spectrometry. Genome Biol. 2005; 6:R9.doi: 10.1186/gb-2004-6-1-r9 [PubMed: 15642101]
88. Deutsch EW. The PeptideAtlas Project. Methods Mol Biol. 2010; 604:285–296. DOI: 10.1007/978-1-60761-444-9_19 [PubMed: 20013378]
89. Bateman NW, Goulding SP, Shulman NJ, Gadok AK, Szumlinski KK, MacCoss MJ, et al. Maximizing Peptide Identification Events in Proteomic Workflows Using Data-Dependent Acquisition (DDA). Molecular & Cellular Proteomics. 2014; 13:329–338. DOI: 10.1074/mcp.M112.026500 [PubMed: 23820513]
90. Mellacheruvu D, Wright Z, Couzens AL, Lambert JP, St-Denis NA, Li T, et al. The CRAPome: a contaminant repository for affinity purification-mass spectrometry data. Nat Methods. 2013; 10:730–736. DOI: 10.1038/nmeth.2557 [PubMed: 23921808]
91. Rellos P, Pike ACW, Niesen FH, Salah E, Lee WH, von Delft F, et al. Structure of the CaMKIIdelta/calmodulin complex reveals the molecular mechanism of CaMKII kinase activation. PLoS Biol. 2010; 8:e1000426.doi: 10.1371/journal.pbio.1000426 [PubMed: 20668654]
92. Huttlin EL, Ting L, Bruckner RJ, Gebreab F, Gygi MP, Szpyt J, et al. The BioPlex Network: A Systematic Exploration of the Human Interactome. Cell. 2015; 162:425–440. DOI: 10.1016/j.cell.2015.06.043 [PubMed: 26186194]
93. Enz R. Metabotropic glutamate receptors and interacting proteins: evolving drug targets. Curr Drug Targets. 2012; 13:145–156. DOI: 10.2174/138945012798868452 [PubMed: 21777188]
94. Petralia RS, Wang Y-X, Sans N, Worley PF, Hammer Iii JA, Wenthold RJ. Glutamate receptor targeting in the postsynaptic spine involves mechanisms that are independent of myosin Va. Eur J Neurosci. 2001; 13:1722–1732. DOI: 10.1046/j.0953-816x.2001.01553.x [PubMed: 11359524]
95. Petralia RS, Sans N, Wang YX, Wenthold RJ. Ontogeny of postsynaptic density proteins at glutamatergic synapses. Mol Cell Neurosci. 2005; 29:436–452. DOI: 10.1016/j.mcn.2005.03.013 [PubMed: 15894489]
96. Phillips GR, Huang JK, Wang Y, Tanaka H, Shapiro L, Zhang W, et al. The presynaptic particle web: ultrastructure, composition, dissolution, and reconstitution. Neuron. 2001; 32:63–77. DOI: 10.1016/S0896-6273(01)00450-0 [PubMed: 11604139]
97. Phillips GR, Florens L, Tanaka H, Khaing ZZ, Fidler L, Yates JR, et al. Proteomic comparison of two fractions derived from the transsynaptic scaffold. J Neurosci Res. 2005; 81:762–775. DOI: 10.1002/jnr.20614 [PubMed: 16047384]
98. Collins MO, Husi H, Yu L, Brandon JM, Anderson CNG, Blackstock WP, et al. Molecular characterization and comparison of the components and multiprotein complexes in the postsynaptic proteome. J Neurochem. 2006; 97:16–23. DOI: 10.1111/j.1471-4159.2005.03507.x [PubMed: 16635246]
99. Distler U, Schmeisser MJ, Pelosi A, Reim D. In-depth protein profiling of the postsynaptic density from mouse hippocampus using data-independent acquisition proteomics. 2014; doi: 10.1002/pmic.201300520

100. Föcking M, Dicker P, Lopez LM, Hryniewiecka M, Wynne K, English JA, et al. Proteomic analysis of the postsynaptic density implicates synaptic function and energy pathways in bipolar disorder. Transl Psychiatry. 2016; 6:e959–9. DOI: 10.1038/tp.2016.224 [PubMed: 27898073]

101. Naisbitt S, Kim E, Tu JC, Xiao B, Sala C, Valtschanoff J, et al. Shank, a novel family of postsynaptic density proteins that binds to the NMDA receptor/PSD-95/GKAP complex and cortactin. Neuron. 1999; 23:569–582. [PubMed: 10433268]

102. Coultrap SJ, Bayer KU. CaMKII regulation in information processing and storage. Trends Neurosci. 2012; 35:607–618. DOI: 10.1016/j.tins.2012.05.003 [PubMed: 22717267]

103. Easton AC, Lucchesi W, Mizuno K, Fernandes C, Schumann G, Giese KP, et al. αCaMKII autophosphorylation controls the establishment of alcohol-induced conditioned place preference in mice. Behav Brain Res. 2013; 252:72–76. DOI: 10.1016/j.bbr.2013.05.045 [PubMed: 23732653]

104. Kendler KS, Kalsi G, Holmans PA, Sanders AR, Aggen SH, Dick DM, et al. Genomewide association analysis of symptoms of alcohol dependence in the molecular genetics of schizophrenia (MGS2) control sample. Alcohol Clin Exp Res. 2011; 35:963–975. DOI: 10.1111/j.1530-0277.2010.01427.x [PubMed: 21314694]

105. Sharma V, Eng JK, MacCoss MJ, Riffle M. A Mass Spectrometry Proteomics Data Management Platform. Mol Cell Proteomics. 2012; 11:824–831. DOI: 10.1074/mcp.O111.015149 [PubMed: 22611296]

Abbreviations

EVH1	Enabled/vasodilator-stimulated phosphoprotein homology 1
PPXXF	Proline-Proline-X-X-Phenylalanine, where X is any amino acid
PXXF	Proline-X-X-Phenylalanine, where X is any amino acid
LPSSP	Leucine-Proline-Serine-Serine-Proline
PSD	Postsynaptic density
WT	Wild-type
KO	Knockout
MS1	Precursor mass spectrum
SRM	Selected reaction monitoring
XIC	Extracted ion chromatogram
ppm	Parts per million
FDR	False discovery rate
co-IP	Co-immunoprecipitation
co-IPed	Co-immunoprecipitated
IP	Immunoprecipitation
IPed	Immunoprecipitated
LTP	Long-term potentiation

HEK-293 Human Embryonic Kidney 293 cells

Highlights

- Homer2 interacts with a limited subset of previously reported interaction partners
- We detected 3 of 31 previously reported Homer2-interactors in the mouse brain
- We detected 15 “novel” Homer2-interactors in the mouse brain
- The majority of Homer2-interactors participate in NMDAR signal transduction

Significance

Homer proteins are scaffolding proteins that regulate signal transduction in neurons. Identifying their interaction partners is key to understanding their function. We used co-immunoprecipitation in combination with mass spectrometry to establish the first comprehensive list of Homer2-interacting partners in the mouse brain. The specificity of interactions was evaluated using Homer2 knockout brain tissue as a negative control. The set of proteins that we identified minimally overlaps with previously reported interacting partners of Homer2. In particular, we identified novel interactors that are part of the signaling cascade activated by glutamatergic transmission, which improves our mechanistic understanding of the role of Homer2 in behavior.

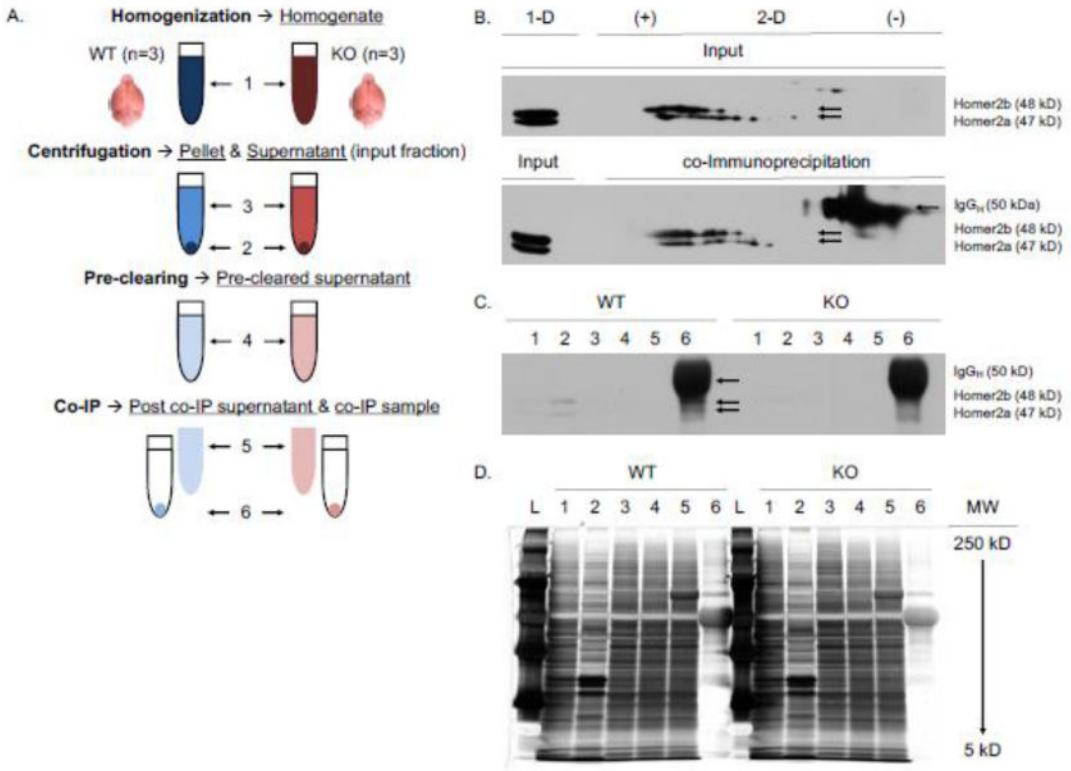

Figure 1. Validation of an anti-Homer2 antibody for co-IP experiments

(A) Workflow of the Anti-Homer2 co-IP experiment. The different WT and KO fractions are colored in blue and red, respectively. (B) 2-D western blot images of a representative input fraction (top) and a representative co-IP sample (bottom) blotted for Homer2a and Homer2b proteins. (C) 1-D western blot image of fractions collected from a representative co-IP experiment performed using WT (left) and KO (right) mouse whole-brain samples and blotted for Homer2 proteins. (D) 1-D silver stained gel image of fractions collected from a representative co-IP experiment performed using WT (left) and KO (right) mouse whole-brain samples. Lanes in (A), (C), and (D) correspond to: (L), ladder; (1), Homogenate; (2), Pellet; (3), Supernatant (input fraction); (4), Pre-cleared supernatant; (5), Post-co-IP supernatant; and (6) co-IP sample. MW = molecular weight

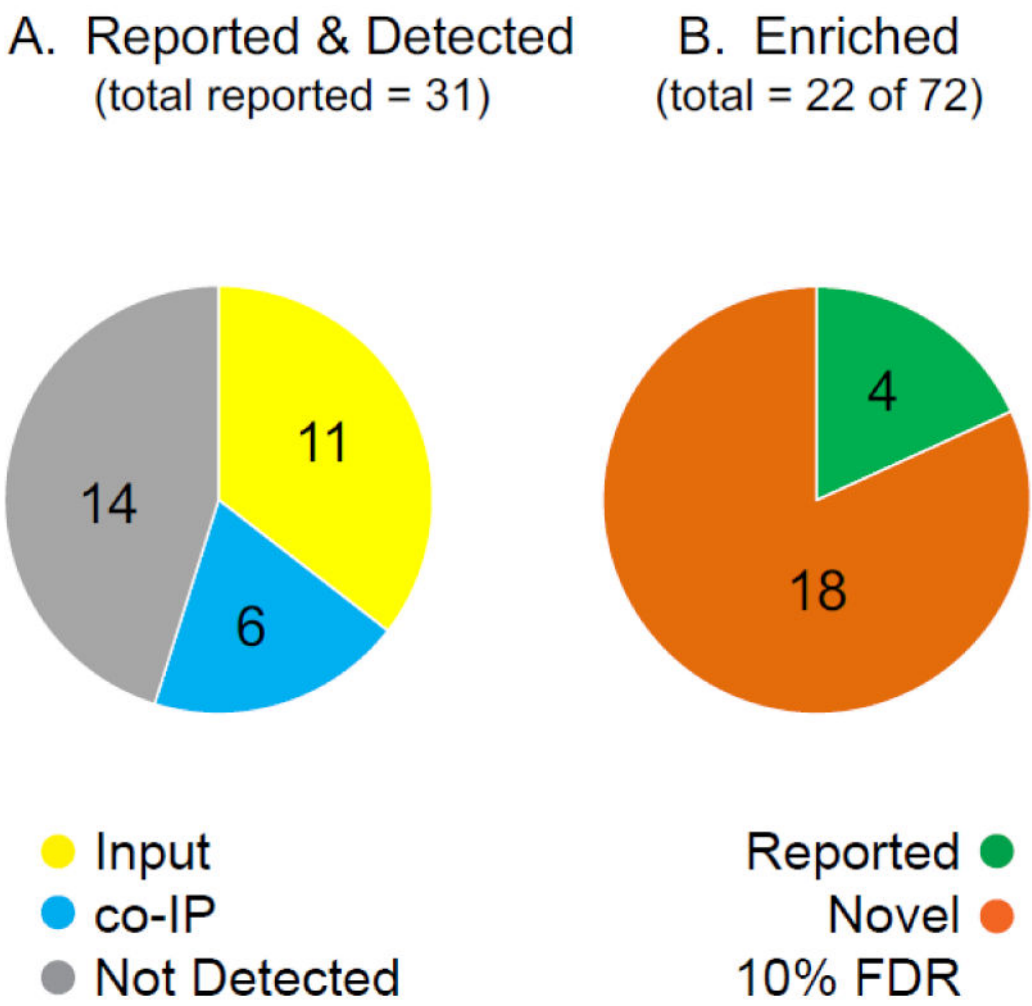

Figure 2. Detection of previously reported and enrichment of novel Homer2-interacting proteins

(A) Of the 31 previously reported Homer2-interacting proteins, 11 were detected by MS1 full-scan filtering in the mouse whole-brain fractions used to co-IP Homer2 (yellow), 6 were detected in the co-IP samples (blue), and 14 proteins were not detected in either dataset (gray). (B) A total of 22 proteins were significantly enriched at a 10% FDR in WT co-IP samples. In addition to the four previously reported Homer2-interacting proteins (green), 18 novel proteins co-IPed with Homer2 (orange). FDR = false discovery rate.

A. Previously Reported Homer2-Interacting Proteins

Detected

Input	Co-IP	UniProt ID	Indistinguishable Group?	Gene	Protein Description	Common Name
		P60710	Yes	*Actb*	Actin, cytoplasmic 1	β-actin
		Q3UHD9	Yes	*Agap2*	Arf-GAP with GTPase, ANK repeat and PH domain-containing protein 2	PIKE
		P12023-3	Yes	*App*	Isoform APP751 of Amyloid beta A4 protein	APP751
		G5E829	No	*Atp2b1*	Plasma membrane calcium-transporting ATPase 1	PMCA1
		E9Q828	Yes	*Atp2b4*	Calcium-transporting ATPase	PMCA4
		P60766	Yes	*Cdc42*	Cell division control protein 42 homolog	CDC42
		B2RX88	N/A	*Cspp1*	Centrosome and spindle pole-associated protein 1	CSPP1
		Q6WQJ1	N/A	*Dagla*	Sn1-specific diacylglycerol lipase alpha	DGL-α
		Q9QXS6	Yes	*Dbn1*	Drebrin	Drebrin
		Q8BZ98	Yes	*Dnm3*	Dynamin-3	Dynamin-3
		O08796	N/A	*Eef2k*	Eukaryotic elongation factor 2 kinase	eEF-2K
		P97772	N/A	*Grm1*	Metabotropic glutamate receptor 1	mGluR1-α
		Q3UVX5	Yes	*Grm5*	Metabotropic glutamate receptor 5	mGluR5
		Q9Z2Y3	Yes	*Homer1*	Homer protein homolog 1	Homer1
		Q9QWW1	Yes	*Homer2*	Homer protein homolog 2	Homer2
		Q99JP6	Yes	*Homer3*	Homer protein homolog 3	Homer3
		Q8BXG3	N/A	*Ift57*	Intraflagellar transport protein 57 homolog	IFT57
		P11881	Yes	*Itpr1*	Inositol 1,4,5-trisphosphate receptor type 1	IP3R1
		P52293	N/A	*Kpna2*	Importin subunit alpha-1	Importin α-P1
		E9PV66	N/A	*Myo18b*	Protein Myo18b	Myo18b
		O88942	N/A	*Nfatc1*	Nuclear factor of activated T-cells, cytoplasmic 1	NFATc1
		Q60591	N/A	*Nfatc2*	Nuclear factor of activated T-cells, cytoplasmic 2	NFATc2
		Q8K120	N/A	*Nfatc4*	Nuclear factor of activated T-cells, cytoplasmic 4	NFATc4
		Q9Z1B3	Yes	*Plcb1*	1-phosphatidylinositol 4,5-bisphosphate phosphodiesterase beta-1	PLC-β-1
		P63001	N/A	*Rac1*	Ras-related C3 botulinum toxin substrate 1	Rac1
		Q9QUI0	No	*Rhoa*	Transforming protein RhoA	RhoA
		E9PZQ0	N/A	*Ryr1*	Ryanodine receptor 1	RyR1
		Q4ACU6	Yes	*Shank3*	SH3 and multiple ankyrin repeat domains protein 3	Shank3
		Q61056	N/A	*Trpc1*	Short transient receptor potential channel 1	TrpC1
		Q922Y1	No	*Ubxn1*	UBX domain-containing protein 1	2B28
		Q9CRC0	N/A	*Vkorc1*	Vitamin K epoxide reductase complex subunit 1	VKORC1

B. Putative Homer2-Interacting Proteins

Enriched

Reported	Novel	UniProt ID	Indistinguishable Group?	Gene	Protein Description	Common Name	FC (log2)	FDR	SRM Verified (+2 peptides)
		Q8BIZ1	Yes	*Anks1b*	Ankyrin repeat and sterile alpha motif domain-containing protein 1B	ANKS1B	2.56	0.04	Yes (1 of 1)
		Q8BW86	Yes	*Arhgef33*	Rho guanine nucleotide exchange factor 33	RhoGEF33	3.46	0.02	Yes (3 of 4)
		Q8BKX1	Yes	*Baiap2*	Brain-specific angiogenesis inhibitor 1-associated protein 2	BAIAP2	2.58	0.03	Yes (2 of 3)
		P11798	Yes	*Camk2a*	Calcium/calmodulin-dependent protein kinase type II subunit alpha	CaMKII-α	1.40	0.08	Yes (6 of 8)
		P28652	No	*Camk2b*	Calcium/calmodulin-dependent protein kinase type II subunit beta	CaMKII-β	1.57	0.07	Yes (4 of 4)
		Q91XM9	Yes	*Dlg2*	Disks large homolog 2	PSD-93	2.33	0.05	No (0 of 2)
		P70175	No	*Dlg3*	Disks large homolog 3	SAP-102	4.09	0.02	No (0 of 2)
		Q62108	Yes	*Dlg4*	Disks large homolog 4	PSD-95	2.81	0.02	Yes (3 of 4)
		Q6A0A9	No	*FAM120A*	Constitutive coactivator of PPAR-gamma-like protein 1	FAM120A	0.44	0.06	No (0 of 4)
		P35438	Yes	*Grin1*	Glutamate receptor ionotropic, NMDA 1	GluN1	2.35	0.02	Yes (2 of 3)
		Q01097	No	*Grin2b*	Glutamate receptor ionotropic, NMDA 2B	GluN2B	3.33	0.02	Yes (1 of 2)
		Q9Z2Y3	Yes	*Homer1*	Homer protein homolog 1	Homer1	1.00	0.03	Yes (10 of 11)
		Q9QWW1	**Yes**	***Homer2***	**Homer protein homolog 2**	**Homer2**	**2.58**	**0.02**	**Yes (3 of 3)**
		Q99JP6	Yes	*Homer3*	Homer protein homolog 3	Homer3	0.27	0.08	Yes (7 of 8)
		Q80TE7	No	*Lrrc7*	Leucine-rich repeat-containing protein 7	LRRC7	2.29	0.05	Yes (2 of 2)
		Q8K411	Yes	*Pitrm1*	Presequence protease, mitochondrial	PITRM1	0.22	0.08	Yes (9 of 11)
		D3YZU1	No	*Shank1*	SH3 and multiple ankyrin repeat domains protein 1	Shank1	3.17	0.02	Yes (3 of 3)
		Q80Z38	Yes	*Shank2*	SH3 and multiple ankyrin repeat domains protein 2	Shank2	2.97	0.02	Yes (2 of 4)
		Q4ACU6	Yes	*Shank3*	SH3 and multiple ankyrin repeat domains protein 3	Shank3	2.77	0.05	Yes (2 of 2)
		Q9QW16	Yes	*Srcin1*	SRC kinase signaling inhibitor 1	SRCIN1	0.40	0.05	Yes (2 of 4)
		F6SEU4	No	*Syngap1*	Ras/Rap GTPase-activating protein SynGAP	SYNGAP1	3.27	0.02	Yes (3 of 3)
		Q8BJH1	Yes	*Zc2hc1a*	Zinc finger C2HC domain-containing protein 1A	ZC2HC1A	0.50	0.06	Yes (3 of 5)

Figure 3. Detection of previously reported and enrichment of novel Homer2-interacting proteins

(A) Detection of previously reported Homer2-interacting proteins in the input fractions and co-IP samples. (B) Enrichment of previously reported and novel Homer2-interacting proteins in co-IP samples. Previously reported Homer2-interacting proteins that were detected in the input fractions and co-IP samples are colored yellow and blue, respectively. Previously reported and novel Homer2-interacting proteins that were significantly enriched in WT samples are colored green and orange, respectively. Table headers correspond to: (UniProt ID), mouse UniProt protein identifier; (Indistinguishable Group), proteins that contain peptides expressed in more than one gene product; (Gene) common gene name; (Protein Description) protein name; (Common Name) short protein name or alternative protein name; (FC Log2) Log2 transformed fold change; (FDR) false discovery rate ($q \leq 0.10$) ; [SRM Verified (+2 peptides)], whether or not the protein was verified by SRM mass spectrometry using +2 charged peptides in a second co-IP experiment. N/A = not applicable.

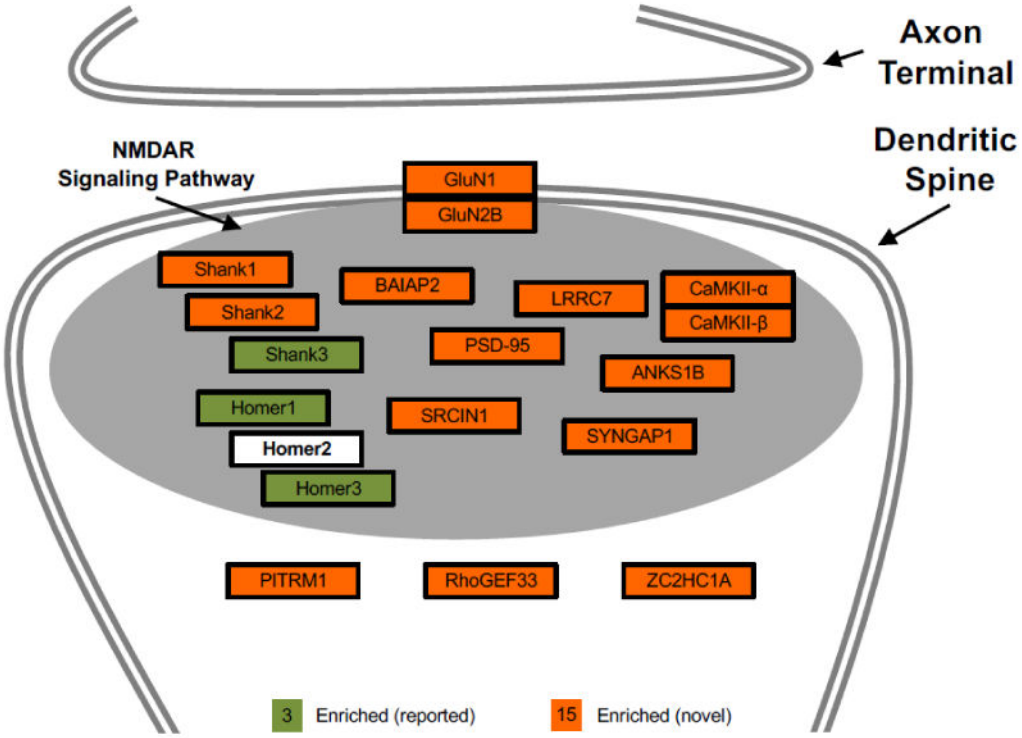

Figure 4. Homer2-interacting proteins in the mouse brain

Cartoon depiction of a neuronal post-synapse. Previously reported Homer2-interacting proteins that were significantly enriched in WT samples are colored green and novel proteins are colored orange. The majority of Homer2-interacting proteins are NMDAR subunits or part of the NMDAR signaling pathway (gray area). Homer2 is not included as an interacting protein because our co-IP experiments cannot differentiate Homer2 proteins directly bound by the antibody from Homer2 homomultimers. Literature references for the involvement of these proteins in the NMDAR signaling pathway are included in Supplemental Table 3.